JOURNAL OF Applied Polymer SCIENCE

Reinforced chloroprene rubber by *in situ* generated silica particles: Evidence of bound rubber on the silica surface

Bharat P. Kapgate,[1] Chayan Das,[1] Amit Das,[2,3] Debdipta Basu,[2] Sven Wiessner,[2,4] Uta Reuter,[2] Gert Heinrich[2,4]

[1]Department of Chemistry, Visvesvaraya National Institute of Technology, Nagpur, India
[2]Leibniz-Institut für Polymerforschung Dresden e.V. Dresden, Germany
[3]Tampere University of Technology, Tampere, Finland
[4]Technische Universität Dresden, Institut Für Werkstoffwissenschaft, Dresden, Germany
Correspondence to: C. Das (E-mail: chayandas@hotmail.com or chnds@rediffmail.com)

ABSTRACT: Nano silica is generated *in situ* inside the uncrosslinked chloroprene rubber (CR) by the sol-gel reaction of tetraethoxysilane (TEOS). This results in appreciable improvement in mechanical properties of the CR composites at relatively low filler content. Furthermore, exploitation of reactive organosilanes, γ-aminopropyltrimethoxysilane (γ-APS) in particular, in the silica synthesis process facilitates growing of spherical silica particles with a size distribution in the range of 20-50 nm. The silica particles are found to be uniformly dispersed and they do not suffer from filler-filler interaction. Additionally, it is observed that the silica particles are coated by silane and rubber chains together which are popularly known as bound rubber. The existence of the bound rubber on silica surface has been supported by the detailed investigations with transmission electron microscopy (TEM), energy filtered transmission electron microscopy (EFTEM) and energy dispersive X-ray spectroscopy (EDAX). The interaction between rubber and silica, via bifunctionality of the γ-APS, has been explored by detailed FTIR studies. © 2016 Wiley Periodicals, Inc. J. Appl. Polym. Sci. **2016**, *133*, 43717.

KEYWORDS: bound rubber; *in situ silica* and silane treatment; transmission electron microscopy

Received 25 September 2015; accepted 3 April 2016
DOI: 10.1002/app.43717

INTRODUCTION

Replacement of conventional reinforcing fillers such as carbon black and silica, which are used in bulk amount in elastomer, by a small amount of nanofiller is of immense interest in the area of elastomeric composites. Consequently, tremendous research activities have been oriented in this direction.[1–3] Silica was focused as an alternative of carbon black, due to its several advantages, in few decades back. The fundamentals of reinforcing mechanism of silica into rubber matrix are very much influenced by the state of silica dispersion into rubber matrix and the interaction between rubber and silica. Silica dispersion and filler network into rubber matrix mostly depends on rubber–filler interaction.[4–7] The concept of bound rubber helps to identify the strength of rubber–filler interaction and consequently the reinforcement effect. Strong affinity of chloroprene rubber (CR) towards silica particles, in externally silica filled CR composite, that arises due to formation of hydrogen bonding between the chlorine atom of CR and surface hydroxyl groups of silica is documented in literature.[8] Also, there are few reports on the improvement of properties of silica filled rubber like NR and EPDM by addition of a small amount of CR owing to strong CR–silica interaction that improves the silica dispersion and mechanical properties of the composites.[9,10] In this context, role of sol–gel derived nanosilica, generated *in situ* in the CR matrix, in improving the silica dispersion and mechanical properties of the CR composites appears to be very promising.[6,11,12]

In the present work, a small amount of nano silica is allowed to grow *in situ* inside the CR matrix and the extent of improvement in the composite properties, relative to unfilled composite, is found to be better than what is reported in literature for similar composites but filled with externally added commercial silica.[8] The significance of this result is that the improvement is brought by much less amount of silica (up to 10 phr) than the amount used in case of externally filled CR–silica composites (30 to 40 phr). Furthermore, this reinforcing effect becomes much more pronounced by treating silica with organosilanes during their *in situ* generation into CR matrix by sol–gel method. It may be noted that organosilanes are well known as

Additional Supporting Information may be found in the online version of this article.

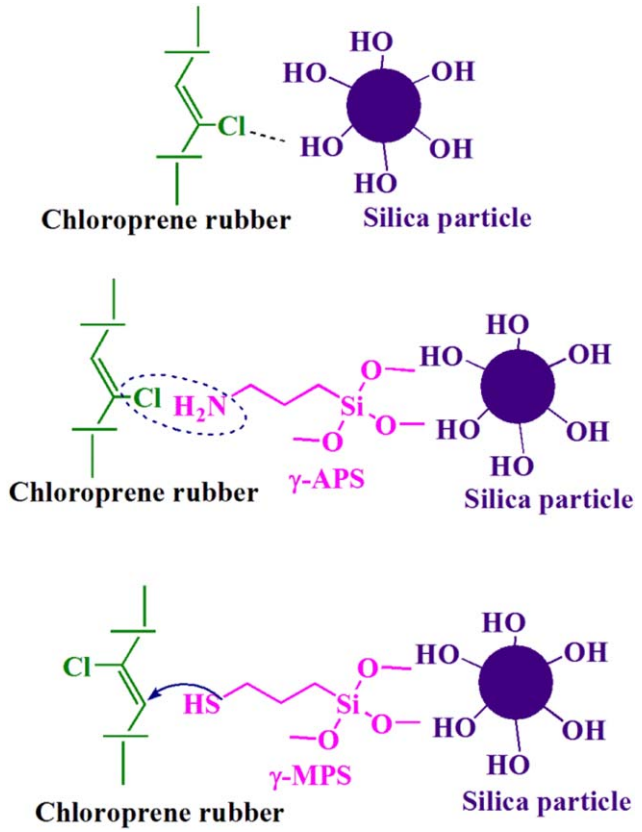

Figure 1. Scheme showing interaction between CR and silica. [Color figure can be viewed in the online issue, which is available at wileyonlinelibrary.com.]

surface modifier of silica and used for the enhancement of surface reactivity of silica towards the rubber matrix. Although many works are reported on the role of silane coupling agents (organosilanes) in enhancing the reinforcement effect of silica for different rubbers, however focus on CR is relatively limited in this regard.[13–18] In the present work, two different trialkoxyorganosilanes viz. γ-aminopropyltrimethoxysilane (γ-APS) and γ-mercaptopropyltrimethoxysilane (γ-MPS), having different functional groups at one of their ends, are employed (Figure 1). Selection of the organosilanes was based on the reactivity of the respective functional groups towards the rubber matrix and it was anticipated that different functionalities of these organosilanes would influence the structural morphology of the silica particles in different ways. It may be mentioned that the existence of a strong interaction between CR and aminosilane was established in the studies on the moisture curing of CR by γ-APS.[19,20] For the other organosilane i.e., γ-MPS, it was believed that the presence of a mercapto group at one of the ends would form linkages with allylic double bonds of CR and would participate in sulfur vulcanization.

It is worthy to mention that the effect of bound rubber on the properties of filled rubber composites has been studied since long. It is a well known fact that the strong rubber–filler interaction leads to the formation of bound rubber content on the surface of filler which may take place via physorption, chemisorption or mechanical interaction.[21] A *bound rubber model* was suggested in several reports where tightly and loosely bound rubber, surrounding the filler particles, had been shown to act as an additional crosslink in the rubber matrix.[22–26] In this study, an effort has been paid to visualise the bound rubber on the surface of the silica particles by detailed morphological investigation.

EXPERIMENTAL

Materials

Chloroprene rubber (LANXESS Baypren 116, XD grade) used in this work was obtained from Heritage Rubber (Nagpur, India). TEOS (Tetraethoxysilane 98%) and n-butylamine were purchased from Acros Organics (New Jersey, USA). Silane coupling agent's viz. γ-MPS (γ–mercptopropyltrimethoxysilane 99%) and γ-APS (γ–aminopropyltrimethoxysilane 99%) were purchased from Aldrich (USA). Tetrahydrofuran (THF) and toluene were purchased from Fischer Scientific (India). Other curatives like sulfur, ZnO (zinc oxide), MgO (magnesium oxide), stearic acid and CBS (N-cyclohexylbenzothiazole-2-sulfenamide) were collected from Sara Polymer Pvt. Ltd. (Nagpur, India). ETU (Ethylene thiourea) was purchased from National chemicals (India).

In Situ Silica Generation into Chloroprene Rubber by Sol–Gel Process

Silica particles were generated and grown *in situ* into unvulcanized CR by sol–gel process. 30 g of CR was dissolved in 400 mL THF and the mixture was stirred by mechanical stirrer till its complete dissolution. Silane coupling agent (γ-APS or γ-MPS) in calculated amount was added for different sample as modifier (formulation given in Table I) and stirred for 1 hour at room temperature for homogeneous mixing. Tetraethoxysilane (TEOS, silica precursor), water and n-butylamine (as a catalyst) were added one by another, where TEOS to water mole ratio was maintained at 1:2 and the catalyst concentration was 0.2 moles with respect to TEOS. The whole mixture was then stirred for 3 hours at room temperature followed by gelation at room temperature for 4 days. Then it was vacuum dried at 50 °C till

Table I. Formulation[a] of Rubber Compounds in phr (Parts by Weight per Hundred Parts of Rubber)

Compound name	Unfilled	In Si-4	In Si-6	In Si-8	In Si-10	In Si-10 + γ-MPS	In Si-10 + γ-APS
CR	100	100	100	100	100	100	100
In situ silica	–	4	6	8	10	10	10
γ-MPS	–	–	–	–	–	1	–
γ-APS	–	–	–	--	–	–	1

[a] Other curatives: ZnO-5; MgO-4; Stearic acid-1; CBS-1; Sulfur-2; ETU-0.5.

constant weight is reached. Amount of TEOS was varied to generate desired content of *in situ* silica for different samples.

Compounding and Vulcanization of *In Situ* Silica Filled Rubber Composites

The curing formulation and silca content of CR composites are given in Table I. Mastication of the *in situ* silica filled CR was done on a two roll mill for 5 minutes followed by compounding with other crosslinking ingredients for another 10 minutes. The unvulcanized sheets were then press cured by compression molding at 160 °C temperature for 25 minutes to obtain vulcanized rubber sheet of 2 mm thickness.

Characterization Techniques

Stress–Strain Studies. Tensile tests of dumbbell shaped samples were carried out using material testing machine (Zwick 1456, Z010, Ulm Germany) with crosshead speed 200 mm/min (ISO 527). Hardness of the composites was determined on Shore A scale by durometer (BSE testing machines, India).

Dynamic Mechanical Analysis. Dynamic mechanical analysis was performed with an Eplexor 2000N dynamic measurement system (Gabo Qualimeter, Ahlden, Germany) using a constant frequency of 10 Hz in a temperature range −100 °C to +140 °C. Analysis was done in the tension mode. For the measurement of the complex modulus, E^*, a static load of 1% prestrain was applied and then the samples were oscillated to a dynamic load of 0.5% strain. Measurements were done with a heating rate of 2 °C/min under liquid nitrogen flow.

Transmission Electron Microscopy. Morphology of composites was studied by transmission electron microscopy (TEM) by ultrathin sections of the samples which was cut by ultramicrotome EM UC6/FC6 (Leica) at about −150 °C and images were obtained using a TEM Libra 200 (Carl-Zeiss) with an acceleration voltage of 200 kV.

Scanning Electron Microscopy. Scanning electron microscopy (SEM) images of the filled composite were obtained by using field emission scanning electron microscope (SEM; Zeiss Ultra Plus; Carl Zeiss Microscopy GmbH, Jena, Germany) equipped with an energy-dispersive X-ray spectrometer (EDX; Quad XFlash 5060, Bruker Corporation, Billerica, MA) at an acceleration voltage of 3 kV. The samples were cut with an ultramicrotome and were sputter coated with 3 nm platinum.

FTIR Spectroscopy. FTIR spectra of prepared rubber samples were recorded in attenuated total reflectance mode (ATR) by Nicolet Magna IR 750, series-II FTIR spectro-photometer. All the measurements were recorded in the scan range of 400 cm^{-1} – 4000 cm^{-1}.

Swelling Studies. Swelling measurements of the composites were carried out by soaking the cured sheet of dimension about (20 × 20 × 2 mm) in toluene for 7 days at room temperature. After each 24 hour, solvent was changed with fresh toluene. Sheets were removed after seven days and solvent on the surface were blotted with blotting paper and weight of the sheets were noted on analytical balance. Degree of swelling (Q) was determined by the following eq. (1).[27]

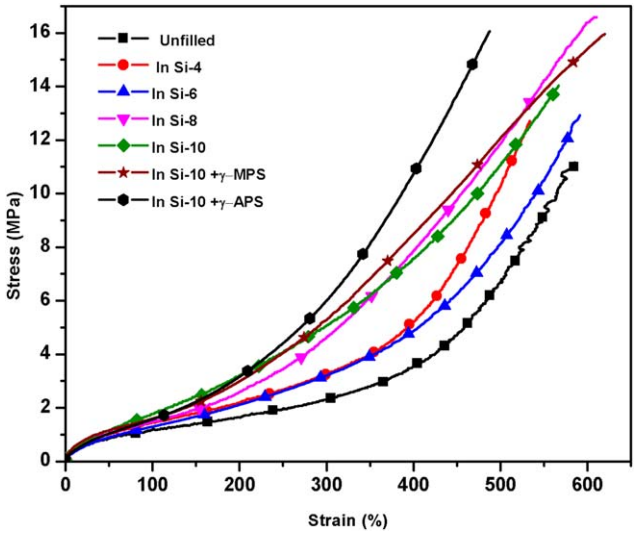

Figure 2. Stress–strain curves of unfilled and filled composites. [Color figure can be viewed in the online issue, which is available at wileyonlinelibrary.com.]

$$Q\ (\%) = (W_s - W_o)/W_o \times 100 \quad (1)$$

where, W_s is the weight of sample after swelling and W_o is the weight of sample before swelling. Crosslink density ν, defined by the number of elastically active chains per unit volume, was measured by Flory-Rehner eq. (2) affine model.[28]

$$\nu = -\left[\ln(1-V_r) + V_r + \chi V_r^2\right]/V_s\left(V_r^{\frac{1}{3}} - V_r/2\right) \quad (2)$$

where, V_s is the molar volume of the toluene (106.2), V_r is the volume fraction of rubber in swollen gel and χ is the Flory-Huggins (CR-Toulene) interaction parameter, which is 0.342 for CR-toluene system.[28]

RESULTS AND DISCUSSION

In general, the state of filler dispersion and rubber–filler interactions play crucial role in influencing the mechanical properties of the elastomeric composites. In this study, silica and CR along with two silane coupling agents viz. γ-APS or γ-MPS have been judiciously selected for the preparation of silica filled CR composites to investigate the direct effect of rubber–filler interaction, brought by *in situ* derived nano silica, on the reinforcement of the CR composites. Indeed, the magnitude of the reinforcing ability of *in situ* silica has been found to be directly dependent on the interaction between rubber and filler. Chemical interactions between CR and silica with and without coupling agent are described in Figure 1. As can be found in Figure 2 and Table II, the stress–strain property of the silica filled CR composites gradually improves with the increase in silica content in the composite. A significant improvement of 100% and 300% modulus values at 10 phr of silica relative to unfilled CR composite is clearly evident. Similarly, shore A hardness values of the *in situ* silica filled composites are found to increase consistently with increase in filler content (Table II). It is worthy to mention here that the reinforcing character of externally added silica (precipitated silica) is generally

Table II. Stress–strain, Hardness and Crosslink Density Values of Unfilled and Filled Composites

Sample Code	Unfilled	In Si-4	In Si-6	In Si-8	In Si-10	In Si-10 + γ-APS	In Si-10 + γ-MPS
$\sigma_{50\%}$ (MPa)	0.90	0.95	0.98	1.05	1.14	1.16	1.19
$\sigma_{100\%}$ (MPa)	1.21	1.31	1.38	1.44	1.74	1.91	1.62
$\sigma_{200\%}$ (MPa)	1.83	2.04	2.28	2.59	3.09	3.92	3.08
$\sigma_{300\%}$ (MPa)	2.48	3.17	3.33	4.52	4.95	7.13	5.35
Tensile strength (MPa)	11.13	12.72	12.92	16.11	13.79	19.41	14.54
Hardness (Shore A)	61	65	66	71	75	72	73
Crosslink density ($\nu \times 10^4$ mol/cc)	1.68	2.51	2.53	2.63	3.01	3.38	3.18

appreciable at relatively higher silica content (30 to 40 phr of silica or even higher) and the system also needs silane coupling agent as reported.[8] But in present case, the reinforcing character of *in situ* derived silica becomes very much significant at relatively lower loading of silica (up to 10 phr) and even without using any silane coupling agent. The improvement in mechanical properties is attributed to the combined effect of strong rubber filler interaction, arising from formation of hydrogen bonds between silanol groups of silica with electronegative chlorine atom present in CR, and increased crosslink density along the series (Table II).[8–10]

A further improvement in the mechanical properties of CR composites is brought by using γ-MPS and γ-APS as coupling agents. It can be observed in Figure 2 that γ-APS improves the stress–strain behavior to a considerable extent whereas the effect of γ-MPS is rather limited at 10 phr silica content. γ-APS treated *in situ* silica filled composite shows much higher modulus and tensile strength over γ-MPS treated *in situ* silica filled composite. This is attributed to the uniform and homogenous dispersion of *in situ* silica as well as a direct grafting of rubber chains on the surface of silica particles in the former case (discussed later). Such adsorption of loosely bound rubber on silica surface via interaction of Cl of CR and free amino group of γ-APS, already grafted on silica surface, results in additional crosslinks (Figure 1, Table II).

To evaluate the reinforcement effect brought by *in situ* silica in CR composite, the enhancement in Young's modulus of the composites (considered at the low strain where linear stress–strain relation is followed) are evaluated according to the modified Guth-Gold equation [eq. (3)].[24–26]

$$\frac{E_c}{E_o} = 1 + 2.5\varphi + 14.1\varphi^2 \qquad (3)$$

where E_c and E_o are the tensile modulus of the filled and unfilled composites respectively. E_c/E_o is termed as the modulus enhancement and φ is the calculated volume fraction of silica in filled composite.

First, the predicted curves for each set, i.e., composites filled with varying amount of untreated, γ-APS treated and γ-MPS treated silica (upto 10 phr) were obtained by putting the calculated φ values in eq. (3). The predicted values are found in the same range for each set of composites. Next, actual modulus enhancement values for each set are plotted against corresponding volume fraction. For this purpose, Young modulus value of each sample (prepared separately) was determined from stress–strain measurement. The experimental values of modulus enhancement (E_c/E_o) are found higher than those of the predicted values for all three sets of composites (Figure 3) and maximum for γ-APS treated silica filled composites. The experimental data are given in Supporting Information Table I. For each set, the curve that fits best to the experimental data was determined by putting optimum value of φ in eq. (3) that has been done by trial and error. Thus, it is found that φ ~ 2, 3 and ~5 for the series of untreated silica, γ-MPS treated silica and γ-APS treated silica filled composites respectively. This clearly suggests that silane treatment of silica enhances the tensile modulus of composites and the influence of γ-APS is more than that of γ-MPS. The value φ ~ 5 for γ-APS treated composites means enhancement in young modulus is much higher than predicted values and the eq. (3) holds good for this series with five times higher the coefficients (2.5 and 14.1) value. So it can be concluded that it is not only the hydrodynamic effect of the rigid filler that causes modulus enhancement but rubber filler interaction and adherence of silane chain on the silica surface, that results in effective increment in volume fraction, also contribute to the modulus enhancement as revealed in this

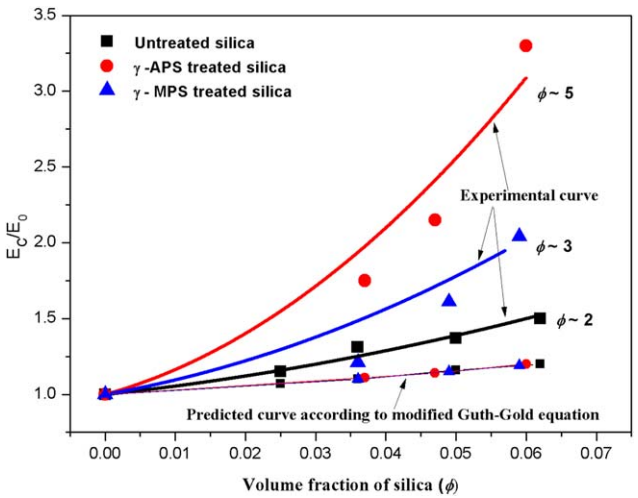

Figure 3. Plots of modulus enhancement (E_c/E_o) versus volume fraction (φ) for both predicted and experimental values for each set viz. untreated silica, γ-APS treated silica and γ-MPS treated silica filled CR. [Color figure can be viewed in the online issue, which is available at wileyonlinelibrary.com.]

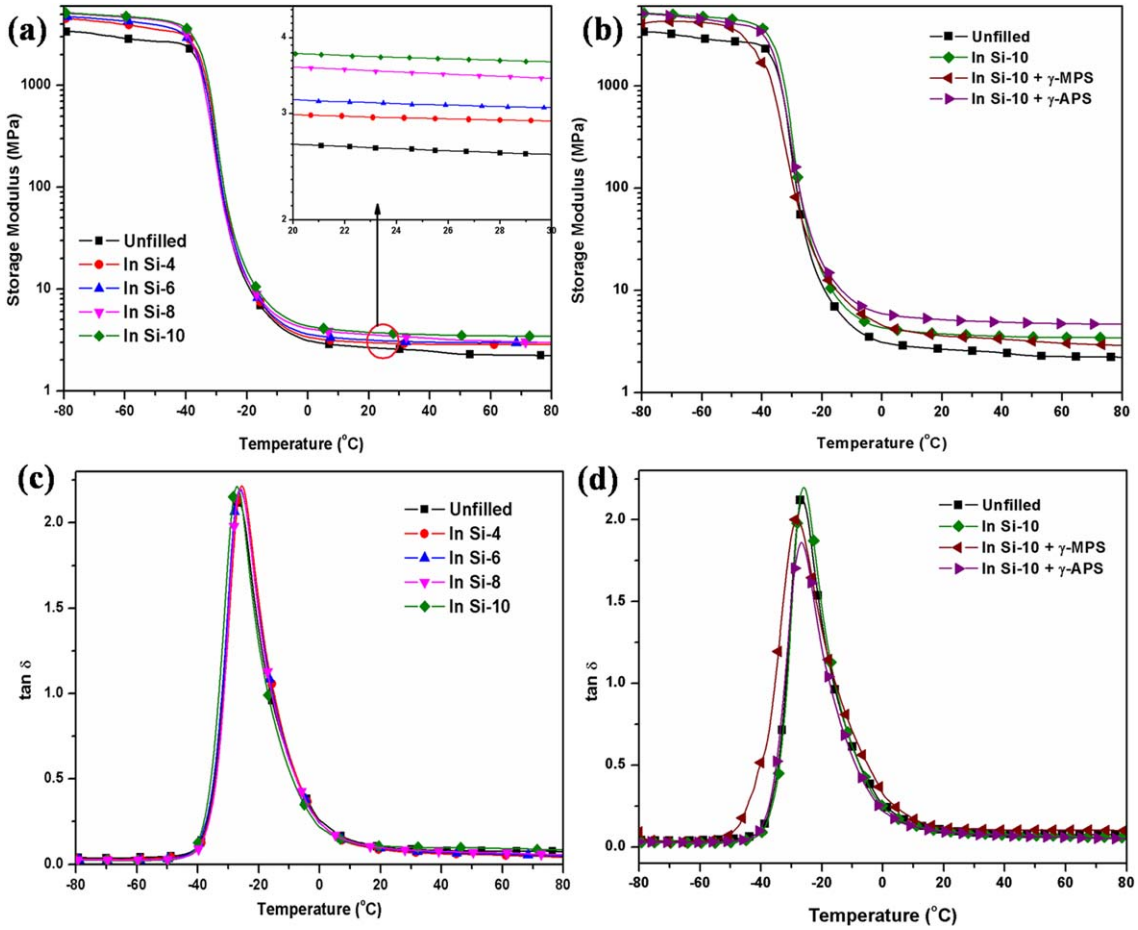

Figure 4. Temperature dependence of (a) storage modulus and (c) tan δ of unfilled and untreated *in situ* silica filled composites at different silica loading, (b) storage modulus and (d) tan δ of unfilled, untreated and silane treated silica filled composites at 10 phr filler content. [Color figure can be viewed in the online issue, which is available at wileyonlinelibrary.com.]

graphical plot. It is reported in literature that the adsorption of polymer chains to the nanofiller interface leads to a higher apparent volume fraction of the swollen particles in the polymer matrix.[30]

Dynamic mechanical behavior of the CR composites, studied against temperature sweep at constant strain and frequency, also supports the superior reinforcing character of *in situ* derived sol–gel silica as observed in stress–strain study. Storage modulus (E') versus temperature plot [Figure 4(a)] shows that silica incorporation causes increase in storage modulus in the rubbery plateau region of the filled composite relative to that of the unfilled one. Moreover, there is gradual increase in the modulus values with the increase in silica content. This indicates better rubber–filler interaction in silica filled composites that arises due to very strong interaction between CR and silica. It may happen that, increase in silica content increases the relative amount of silanol groups on the silica surface. This increases the interacting sites of silica with CR. As a result, stronger rubber–filler interaction and higher crosslink density are developed with increase in silica content that restricts the segmental mobility of the rubber chains and leads to higher storage modulus values. Effect of silanes (γ-MPS and γ-APS) on the dynamic mechanical properties of 10 phr *in situ* silica filled composites is depicted in Figure 4(b). The results reveal that further increase in storage modulus is brought by the treatment with γ-APS while the effect of γ-MPS is not so significant in this regard. This clearly indicates that γ-APS treatment of silica results in further improvement in rubber–filler interaction. This is also reflected in direct grafting of rubber chains on the surface of silica particles in morphological study (discussed later). Increase in crosslink density for this composite also contributes towards storage modulus enhancement as well. The results matches very well with the highest tensile modulus ($\sigma_{100\%}$ and $\sigma_{300\%}$) observed for this composite in stress–strain study. The glass transition temperature (T_g) of the silica filled composites, as observed in the tan δ vs. temperature plot [Figure 4(c–d)], remains almost unaltered with respect to that of unfilled composite. Such findings are reported for reinforced CR[11] and styrene-butadiene-rubber (SBR)[31] where T_g of the composites are found to remain unaffected by the presence of silane coupled silica particles. However, for the composite with γ-APS integrated *in situ* silica, maximum reduction in tan δ peak height is observed. This signifies the better reinforcement effect and strong rubber–filler interaction for this composite.[32,33] This is attributed to the increased crosslink density, unifom distribution of fine spherical silica particles throughout the rubber

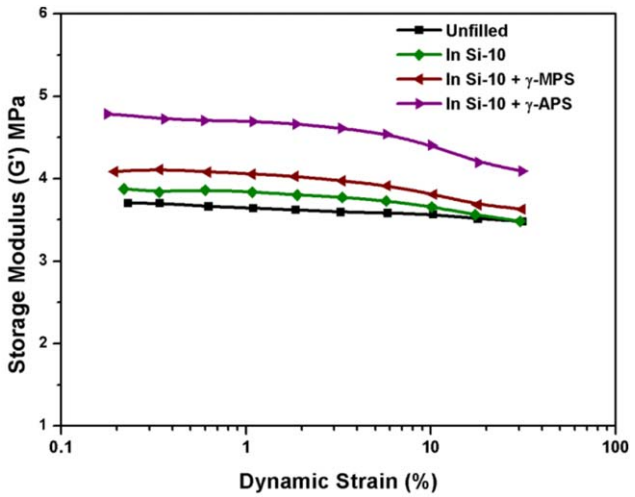

Figure 5. Dependence of storage modulus on dynamic strain of different CR-*in situ* silica nanocomposites. [Color figure can be viewed in the online issue, which is available at wileyonlinelibrary.com.]

matrix in addition to coating of silane over the silica surface which improves the rubber–filler interaction and constrains the rubber chain mobility (confirmed in subsequent studies).

Figure 5 shows the plots of dynamic storage modulus over dynamic strains. In general, a strong dependency of storage modulus over the dynamic strain suggests occurrence of a strong filler–filler network (Payne effect) in a highly filled system. However, as in the present case the amount of silica (volume fraction) is much smaller, the filler–filler network is expected to persist in a local area and not throughout the matrix. From Figure 5, it could be noted that the strain dependency of the dynamic modulus (Payne Effect) is not very prominent indicating poor filler–filler network of the silica. Furthermore, it is observed that the relative positions of the dynamic modulus among the different filler systems are very much dependent on the type of silica and silane coupling chemistry. The higher dynamic modulus indicates higher reinforcing character of the fillers which is governed by the enhancement of higher effective volume fraction of the fillers. This can be explained if the hydrodynamic effect of the silica sphere is stronger as compared with normal silica. In other words, when the bound rubber on the silica surface is thicker the effective volume fraction of the silica is increased. Relatively higher dynamic modulus of γ-APS treated silica system clearly indicates more reinforcing character of the silica, in this case, which is also corroborating the other observations, noted earlier.[29]

Morphology of the CR composites at 10 phr silica loading was studied by TEM. Figure 6(a) shows the presence of spherically shaped silica particles of different size in the CR matrix filled with untreated *in situ* silica. Some particles with finer structure with a dimension of few nm can also be found. The size of the smaller particles lies in the range 40-70 nm, whereas the large

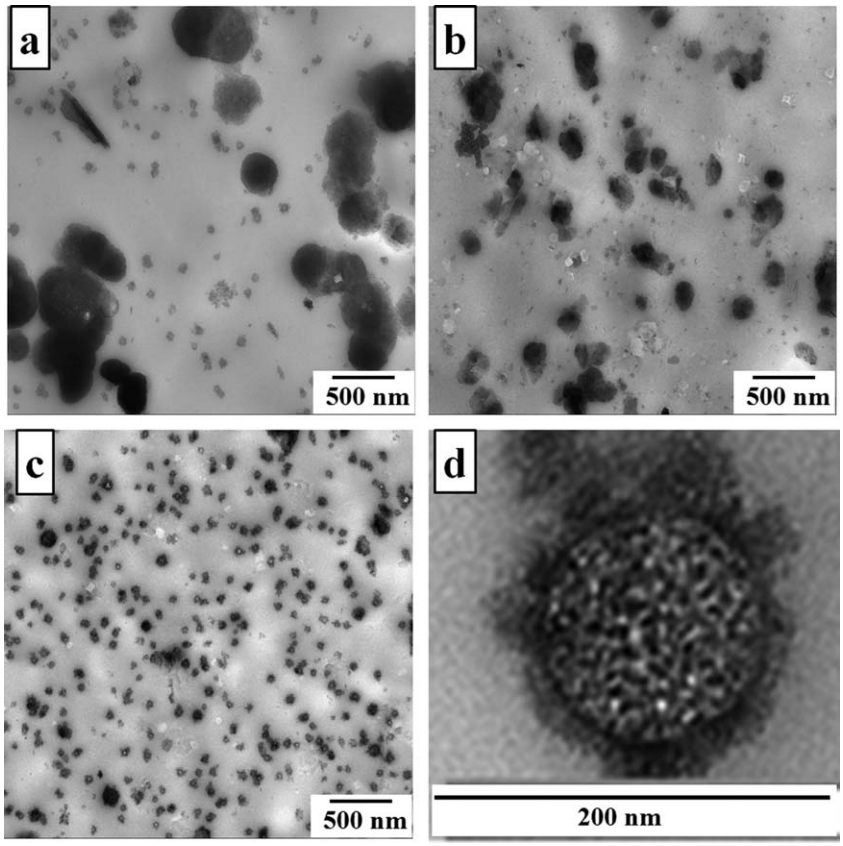

Figure 6. TEM images of CR nanocomposites with 10 phr of Silica (a) Untreated *in situ* silica, (b) *in situ* silica + γ-MPS, (c) *in situ* silica + γ-APS, (d) Close view of TEM image showing single silica particle with adsorbed rubber chains (*in situ* silica + γ-APS).

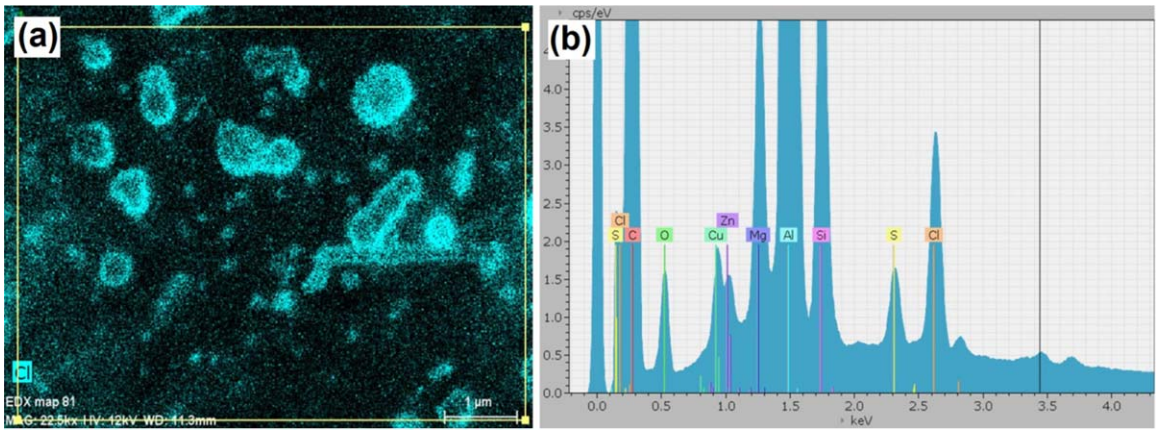

Figure 7. (a) Chlorine mapped SEM EDS image and (b) EDAX pattern of untreated *in situ* silica filled CR composite at 10 phr. [Color figure can be viewed in the online issue, which is available at wileyonlinelibrary.com.]

silica aggregates are of 200–500 nm size. Silane integration of silica in reactive sol–gel method influences the size of silica particles remarkably. A reduction in the agglomeration as well as in the size of silica particles is evident in both γ-APS and γ-MPS based systems. In γ-MPS treated composite, smaller particles show the size distribution in the range of 30-50 nm and larger aggregates in the range of 100–200 nm [Figure 6(b)]. Notably, reduction in particle size and agglomeration are much more pronounced in case of γ-APS system, where the shape and the size of silica particles are found to be more uniform with the narrower size distribution ranging around 20-50 nm [Figure 6(c)]. This suggests that different functionality of two organosilanes (γ-APS and γ-MPS) and their chemistry with the rubber matrix play an important role in tuning the final structure of the silica particles.[34,35] In case of γ-APS, most probably, the presence of basic amino group increases the rate of hydrolysis and condensation of TEOS (silica precursor) that contributes to better filler dispersion with simultaneous reduction in size.[35] A more critical inspection to one of the enlarged image [Figure 6(d)] of γ-APS treated silica filled composite reveals very distinct features of the silica particles with a hard core and diffused shell morphology. It can be assumed that the rubber chains are adsorbed on the surface of hard silica particles due to very strong rubber–filler interaction via bridging γ-APS and form a layer type arrangement surrounding the spherical silica particle. This also helps in preventing the self assembling of silica particles to form large aggregates into rubber matrix.

Increase in bound rubber content (for CR) after external modification of silica by γ-APS is reported in literature although existence of bound rubber is not visualized by detailed morphological study.[13] To establish the existence of bound rubber over silica surface, scanning electron microscopy equipped with energy dispersive X-ray spectroscopy (SEM EDS) was performed for a selected sample (untreated) and the results are shown in Figure 7. It is evident here that the chlorine (Cl) atom is uniformly distributed over the rubber matrix. It can also be seen that the outer surface of the silica particles appears to be brighter compared to the core part of the silica particles. This indicates the presence of chlorine atom on the outer surface of silica particles and suggests that the CR chains are adsorbed on the silica surface. This is attributed to the strong interaction between chlorine atom of CR and surface silanols of silica (Figure 1). More details are given in FTIR discussion.

The coating of organosilane over silica surface present in the *in situ* silica filled γ-APS treated CR matrix is further evidenced by EFTEM study. A zero loss image, obtained from EFTEM study, of γ-APS treated CR – *in situ* silica filled composite at 10 phr, [Figure 8(a)] shows the presence of rough edged spherical silica particles uniformly distributed in the rubber matrix. The elemental mapping of C, O, and Si atoms are shown in Figure 8(b,c,d) respectively. In the C mapped image, the denser (dark) regions around the surface of silica particles (core) indicate that the carbon atoms are uniformly covered over the silica particles.[36] Furthermore, O mapping and Si mapping clearly show appearance of brighter region at the same location, in addition to center core region.[37] So, the presence of C atom in combination with Si and O atoms on the surface of the silica particles suggests the presence of organosilane (i.e., C, O and Si atom from γ-APS) on the surface of silica particles. This reveals the core and shell morphology of the silica particles, where core silica particles are surrounded by a thin layer of silane. Such coating of silane derived by the *in situ* surface modification of silica in the reactive sol–gel system is expected to play a crucial role in enhancing the rubber–silica interaction and the mechanical properties of the composites.

Here we would like to add that it has been a matter of challenge and controversy to give a direct support in favor of the existence of a thin rubber layers on the surface of solid particles as far as the concept of bound rubber and related chain dynamics are concerned. In several literatures the dynamics of such relatively rigid glassy like layers are discussed.[22–26] Nevertheless, in present case the existence of such rubber chains on the silica surface is directly evidenced through detailed morphological investigation.

Strong interaction between CR and silica via γ-APS, that causes adsorption of rubber chain on silica surface, is established by FTIR analysis. FTIR spectrographs of the pure CR, γ-APS treated silica filled CR and γ-MPS treated silica filled CR samples without any crosslinking additives are shown in Figure 9 and the characteristics bands are given in Table III. The IR

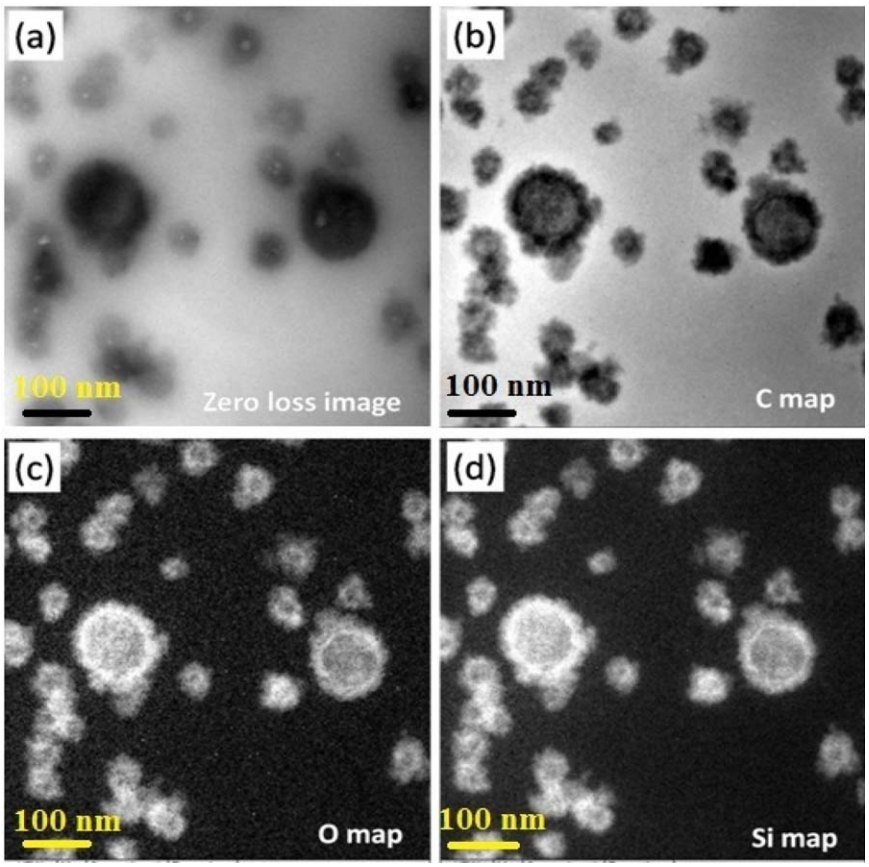

Figure 8. Energy Filtered Transmission Electron Microscopy (EFTEM) images of γ-APS treated CR – *in situ* silica filled composite at 10 phr: (a) Zero loss image; (b) C map image; (c) O map image and (d) Si map image. [Color figure can be viewed in the online issue, which is available at wileyonlinelibrary.com.]

spectrum of γ-APS treated CR sample shows additional peaks at 1580 cm^{-1} (N—H bending), 680 cm^{-1} (N—H wagging) and 1110 cm^{-1} (C—N stretching) with reference to IR spectra of others. Bands around 1100-1000 cm^{-1} (Si—O—Si stretching) derived from γ-APS are also noted.[38] Furthermore, the intensity of the bands at 670 cm^{-1} and 550 cm^{-1} (C—Cl stretching) and at 485 cm^{-1} (C—Cl in-plane bending) is diminished in case of γ-APS treated CR, as compared to those of pure CR.[39] These results confirm the existence of strong interaction between γ-APS and CR that arises via chlorine of CR and amine group of γ-APS. γ-MPS treated CR compound shows almost similar spectra as that of pure CR, except appearance of extra bands at 1100 cm^{-1} due to Si—O—Si stretching and broad peak in the range 3200 cm^{-1} to 3550 cm^{-1} due to stretching of silanol (—OH).[34] So, in this case, there is no such interaction with CR as found in case of γ-APS.

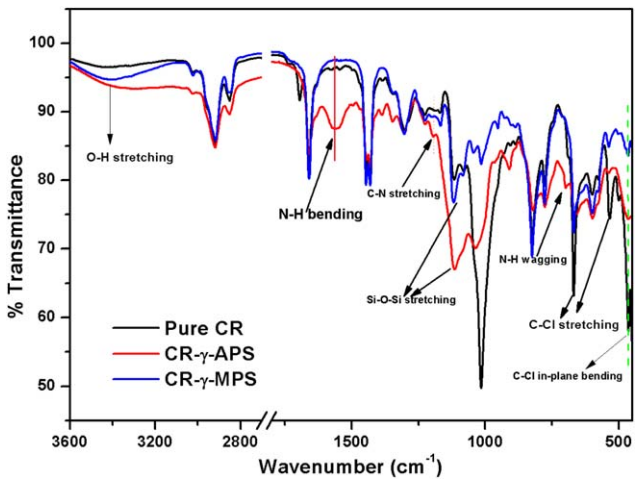

Figure 9. FTIR spectrographs of the pure CR, γ-APS treated CR and γ-MPS treated CR. [Color figure can be viewed in the online issue, which is available at wileyonlinelibrary.com.]

Table III. Characteristics Absorption Peaks in FTIR Spectra[38,39]

Wavenumber	Assignment of peaks
485 cm^{-1}	C—Cl in-plane bending
670 cm^{-1}, 550 cm^{-1}	C—Cl stretching
3200 cm^{-1} to 3550 cm^{-1}	Stretching of silanol (O—H group)
1100 cm^{-1}	Si—O—Si stretching
680 cm^{-1}	N—H wagging
1580 cm^{-1}	N—H bending
1110 cm^{-1}	C—N stretching vibration

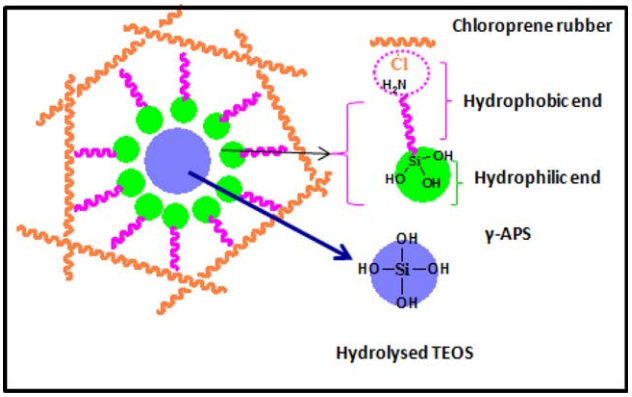

Figure 10. Schematic representation of the inverse micelle formation for silica generation. [Color figure can be viewed in the online issue, which is available at wileyonlinelibrary.com.]

The formation of well defined spherical silica particles into γ-APS treated silica filled CR matrix can be explained on the basis of inverse micelle formation.[12,40] The reaction between chlorine atom of CR and amine group of γ-APS results in the formation of γ-APS modified CR. This increases the length of hydrocarbon chain of γ-APS at one side (hydrophobic end). On the other side of γ-APS, it has hydrolyzable trimethoxy groups which after hydrolysis increase its polarity (hydrophilic end). Thus, γ-APS treated CR can behave like a surfactant and takes part in inverse micelle formation. In rubber solution, hydrolyzed TEOS and water molecules form the core part of the micelle while γ-APS treated CR chain, as a surfactant, forms a surface layer of the micelle, facing the polar hydrolyzed trimethoxy groups (hydroxyl) towards the centre of the micelle as depicted in Figure 10. Eventually, hydrolyzed TEOS and hydrolyzed trimethoxy (hydroxyl) groups of γ-APS get condensed to form solid silica particles.[40] As a result, γ-APS treated CR chain gets coated over the silica surface as observed in morphological study [Figure 6(d)]. Such formation of a reverse micelle plays a vital role in controlling the spherical morphology of the silica particles which is schematically presented in Figure 10.

CONCLUSIONS

Finely dispersed nano silica is generated *in situ* into CR matrix that brings appreciable improvement in mechanical properties at much lower silica content (6-10 phr) in comparison to reported results with externally silica filled composites (30-40 phr). This is attributed to uniform silica dispersion, strong silica–CR interaction and increased crosslinking density as revealed from morphological investigation, dynamic mechanical analysis and swelling studies. Further improvement in silica dispersion, composite properties and rubber–filler interaction is brought by *in situ* silane treatment of silica, with γ-APS in particular. FTIR study establishes the strong CR–silica interaction brought by bifunctionality of γ-APS. TEM picture of γ-APS treated silica filled composite, at higher resolution, shows that the silane and rubber chains are adsorbed on the surface of hard silica particles and forms a layer type arrangement surrounding it. The coating of bound rubber via organosilane over silica surface is directly evidenced by SEM EDS and EFTEM studies. Thus, γ-APS appears to be an efficient surface modifier for silica particles, when employed during *in situ* silica generation in CR matrix by sol–gel process, in controlling the spherical morphology of the particles in the nano range. Proper formulation of such system comprising CR and silica with varying dosage of appropriate silane, could be very effective in delivering the improved composite properties.

ACKNOWLEDGMENTS

B. P. Kapgate thanks VNIT for fellowship assistance.

REFERENCES

1. Thomas, S.; Ranimol, S. Rubber Nanocomposites: Preparation, Properties and Applications; John Wiley and Sons, **2010**.
2. Mittal, V.; Kim, J. K.; Pal, K. Recent Advances in Elastomeric Nanocomposites; Springer, **2011**.
3. Visakh, P. M.; Thomas, S.; Chandra, A. K.; Mathew, A. P. Advances in Elastomers II Composites and Nanocomposites; Springer, **2013**.
4. Wahba, L.; D'Arienzo, M.; Donetti, R.; Hanel, T.; Scotti, R.; Tadiello, L.; Morazzoni, F. *RSC Adv.* **2013**, *3*, 5832.
5. Scotti, R.; Wahba, L.; Crippa, M.; D'Arienzo, M.; Donetti, R.; Santo, N.; Morazzoni, F. *Soft Matter* **2012**, *8*, 2131.
6. Sunada, K.; Takenaka, K.; Shiomi, T. *J. Appl. Polym. Sci.* **2005**, *97*, 1545.
7. Ikeda, Y.; Poompradub, S.; Morita, Y.; Kohjiya, S. *J. Sol-Gel Sci. Technol.* **2008**, *45*, 299.
8. Sae-oui, P.; Sirisinha, C.; Thepsuwan, U.; Hatthapanit, K. *Eur. Polym. J.* **2007**, *43*, 185.
9. Choi, S. S. *J. Appl. Polym. Sci* **2002**, *83*, 2609.
10. Das, A.; Debnath, S. C.; De, D.; Basu, D. K. *J. Appl. Polym. Sci.* **2004**, *93*, 196.
11. Bansod, N. D.; Kapgate, B. P.; Das, C.; Basu, D.; Debnath, S. C.; Roy, K.; Wiessner, S. *RSC Adv.* **2015**, *5*, 53559.
12. Kapgate, B. P.; Das, C. *RSC Adv.* **2014**, *4*, 58816.
13. Siriwong, C.; Sae-Oui, P.; Sirisinha, C. *Polym. Test.* **2014**, *38*, 64.
14. Sae-oui, P.; Sirisinha, C.; Thepsuwan, U.; Hatthapanit, K. *Eur. Polym. J.* **2006**, *42*, 479.
15. Reuvekamp, L. A. E. M.; TenBrinke, J. W.; Van Swaaij, P. J.; Noordermeer, J. W. M. *Rubber Chem. Technol.* **2002**, *75*, 187.
16. Brinke, J. T.; Debnath, S. C.; Reuvekamp, L. A. E. M.; Noordermeer, J. W. M. *Compos. Sci. Technol.* **2003**, *63*, 1165.
17. Kapgate, B. P.; Das, C.; Basu, D.; Das, A.; Heinrich, G.; Reuter, U. *J. Appl. Polym. Sci.* **2014**, *131*, DOI:10.1002/app.40054.
18. Kapgate, B. P.; Das, C.; Basu, D.; Das, A.; Heinrich, G. *J. Elast. Plast.* **2015**, *47*, 248.
19. Yamashita, S; Nakawaki, Y.; Kidera, *Die Makromolekulare Chemie* **1987**, *188*, 2553.

20. Ikeda, Y.; Hashim, A. S.; Kohjiya, S. Bulletin of the Institute for Chemical Research, Kyoto University **1995**, *72*, 406.
21. Choi, S. S. *Polym. Test* **2002**, *21*, 201.
22. Sridhar, V.; Gupta, B. R.; Tripathy, D. K. *J. Appl. Polym. Sci.* **2006**, *102*, 715.
23. Zhang, X.; Loo, L. S. *Macromolecules* **2009**, *42*, 5196.
24. Yang, J.; Han, C. R. *J. Phys. Chem. C* **2013**, *117*, 20236.
25. Qu, M.; Deng, F.; Kalkhoran, S. M.; Gouldstone, A.; Robisson, A.; Van Vliet, K. J. *Soft Matter* **2011**, *7*, 1066.
26. Tadiello, L.; D'Arienzo, M. D.; Credico, B.; Hanel, T.; Matejka, L.; Mauri, M.; Morazzoni, F.; Simonutti, R.; Spirkova, M.; Scotti, R. *Soft Matter* **2015**, *11*, 4022.
27. Sperling, L. H. Introduction to Physical Polymer Science; John Wiley & Sons: New York, **2005**.
28. Ibarra, L.; Chamorro, C. *J. Appl. Polym. Sci.* **1991**, *43*, 1805.
29. Rooj, S.; Das, A.; Stöckelhuber, K. W.; Wang, D. Y.; Galiatsatos, V.; Heinrich, G. *Soft Matter* **2013**, *14*, 3798.
30. Bhattacharya, S. N.; Gupta, R. K.; Kamal, M. R. Polymeric Nanocomposites; Carl Hanser Verlag GmbH & Co.: Munich, **2008**.
31. Robertson, C. G.; Lin, C. J.; Bogoslovov, R. B.; Rackaitis, M.; Sadhukhan, P.; Quinn, J. D.; Roland, C. M. *Rubber Chem. Technol.* **2011**, *84*, 507.
32. Murakami, K.; Iio, S.; Ikeda, Y.; Ito, H.; Tosaka, M.; Kohjiya, S. *J. Mater. Sci.* **2003**, *38*, 1447.
33. Kumnuantip, C.; Sombatsompop, N. *Mater. Lett.* **2003**, *57*, 3167.
34. Scotti, R.; Wahba, L.; Crippa, M.; D'Arienzo, M.; Donetti, R.; Santo, N.; Morazzoni, F. *Soft Matter* **2012**, *8*, 2131.
35. Rahman, I. A.; Jafarzadeh, M.; Sipaut, C. S. *Ceram. Int.* **2009**, *35*, 1883.
36. Horiuchi, S.; Horie, S.; Ichimura, K. *ACS Appl. Mater. Inter* **2009**, *1*, 977.
37. Dohi, H.; Horiuchi, S. *Langmuir* **2007**, *23*, 12344.
38. Vansant, E. F.; Van Der Voort, P.; Vrancken, K. C. Characterization and Chemical Modification of the Silica Surface; Elsevier Science B.V.: Amsterdam, **1995**.
39. Sathasivam, K.; Haris, M.; Mohan, S. *Int. J. Chem. Tech. Res.* **2010**, *2*, 1780.
40. Miloskovska, E.; Hansen, M. R.; Friedrich, C.; Hristova-Bogaerds, D.; Van Duin, M. D.; With, G. *Macromolecules* **2014**, *47*, 5174.